Jelena Petrović
Živojin Stamenković
Jasmina Bogdanović-Jovanović
Milica Nikodijević ✉
Miloš Kocić
Dragiša Nikodijević

https://doi.org/10.21278/TOF.463036021
ISSN 1333-1124
eISSN 1849-1391

ELECTRO-MAGNETOCONVECTION OF CONDUCTIVE IMMISCIBLE PURE FLUID AND NANOFLUID

Summary

This paper discusses the magnetohydrodynamic flow and heat transfer in a horizontal channel whose top and bottom halves have different or the same permeability. The top half of the channel is saturated with oil and the bottom half with a water-based nanofluid. The channel is under the influence of an external homogeneous vertical magnetic field and an external homogeneous electric field perpendicular to the vertical longitudinal plane of the channel. The Darcy model is used to determine the fluid flow and heat transfer. Expressions for velocity and temperature distributions are defined and presented graphically for different values of the dimensionless parameters. The Nusselt numbers are determined and given in a table. The paper also investigates the influence of the Hartmann number, the porosity factor, the electrical load factor and the volume fraction of the nanofluid on velocity and temperature distributions in the channel as well as the Nusselt numbers. It has been shown that an increase in the volume fraction of nanoparticles leads to a decrease in the temperature in the channel. Increasing the porosity factor reduces the fluid velocity in the channel and increases the temperature. The Hartmann number increases the temperature in the channel. Higher absolute values of the load factor correspond to higher temperatures. By changing the value of this factor, the direction of fluid flow can also be changed.

Key words: *nanofluid, magnetic field, electric field, porous medium, heat transfer*

1. Introduction

Convection flow and heat transfer of an electrically conductive fluid in channels with a magnetic and an electric field have a wide application in magnetohydrodynamics, in particular with regard to pumps, generators, accelerators, flow gauges, nuclear reactors, geothermal systems, etc. Numerous problems addressed by plasma physics, aeronautics, geophysics, oil industry, etc. involve the flow of multiple layers of different fluids. The common goal regarding all these problems is to improve heat transfer. A good way to improve heat transfer

is to use porous media with a metal matrix. Saturated porous media are commonly used, which requires that their pores be open, interconnected, and completely filled with a fluid so that it is able to flow. Darcy conducted and published the first studies of transport phenomena in a porous medium as early as 1856 [1].

Nomenclature

u – fluid velocity,
T – fluid temperatures,
K – permeability,
k – thermal conductivity,
1 and 2 – subscripts to the base fluid,
f, s, and nf – subscripts to the base fluid, the nanoparticles and the nanofluid, respectively,
E – electric field,
B – magnetic induction,
T_{w1} – temperature of the top plate,
T_{w2} – temperature of the bottom plate,
$Ha = Bh\sqrt{\frac{\sigma_1}{\mu_1}}$ – Hartmann number,
$K = \frac{E}{BU_0}$ – electrical load factor,
$Br = \frac{\mu_1 U_0^2}{k_1\left(T_{w1} - T_{w2}\right)} = \Pr Ec$ – Brinkman number,
$\Pr = \frac{\mu_1 c_{p1}}{k_1}$ – Prandtl number,
$Ec = \frac{U_0^2}{c_{p1}\left(T_{w1} - T_{w2}\right)}$ – Eckert number,

Greek symbols

ρ – density,
μ – viscosity,
σ – electrical conductivity,
ϕ – volume fraction of nanoparticles,
$\Lambda_1 = \frac{h^2}{K_1}$ – porosity factor,
$\Lambda_2 = \frac{h^2}{K_2}$ – porosity factor.

A more recent way to improve heat transfer is to utilize nanofluids. Such fluids contain solid particles (nanoparticles) with a typical length of $1-50$ nm. The first studies on nanofluids were presented by Choi at the ASME winter annual meeting in 1995 and subsequently published [2]. In recent years, the use of porous media with nanofluids has attracted considerable attention, resulting in extensive research in the field of heat and mass transfer.

After the publication of the textbook on magnetohydrodynamics by Shercliff in 1965 [3], many researchers began to study the magnetohydrodynamic (MHD) fluid flow and heat transfer, with the principal focus on the influence of magnetic field on heat and mass transfer and its use to manage these phenomena. There is growing research on heat and mass transfer during the MHD flow of nanofluids in porous media. According to Das et al. [4], several hundred research teams throughout the world studied nanofluids in 2007, and there are probably many more such teams today. The majority of these studies are accessible to the scientific and professional community.

Thus, Wang and Mujumdar [5] reviewed the studies on convection flows and heat transfer of nanofluids and put forward some suggestions for further research. Umavathi et al. [6] studied the unsteady MHD flow and heat transfer of two immiscible fluids in a horizontal channel with an applied homogeneous vertical magnetic field. In the paper by Nikodijević et al. [7], the nonstationary MHD flow and heat transfer in a horizontal channel are considered. The medium in the channel is porous. The external magnetic field is inclined with respect to the channel walls. Gorla and Chamka [8] investigated the natural convective boundary layer

flow over a horizontal plate in a porous medium saturated with a nanofluid. Raju and Rao [9] investigated the electro-magnetohydrodynamic (EMHD) flow and heat transfer of two immiscible fluids in a horizontal channel. Hall currents where also taken into account.

Khalili et al. [10] numerically analysed the unsteady MHD flow and heat transfer of a nanofluid over a sheet stretching/shrinking near the stagnation point. The sheet was immersed in a porous saturated medium and the applied magnetic field was homogeneous and perpendicular to the sheet. Das et al. [11] investigated the generation of entropy in the MHD pseudo-plastic nanofluid flow through a vertical porous channel with convective heating and an applied transverse magnetic field. Das et al. [12] also investigated a fully developed mixed convective flow of nanofluids in a vertical channel with an applied homogeneous transverse magnetic field and an induced magnetic field. Lima et al. [13] investigated the MHD flow and heat transfer of two immiscible fluids in an oblique channel between parallel plates. The effects of the porous layers, buoyancy, Joule and viscous heating, the moving plate, the inclined magnetic field and heat generation/absorption were considered. Manjet and Sharma [14] investigated the MHD flow and convective heat transfer of a Newtonian fluid and a nanofluid that are immiscible in the horizontal channel. The influences of different physical parameter on velocity, temperature, Nusselt number and skin friction coefficient were studied. Petrović et al. [15] studied the MHD flow and heat transfer of two immiscible fluids in a porous saturated medium between horizontal plates at different temperatures. The external magnetic field was homogeneous and inclined in relation to the flow direction and the electric field was homogeneous and perpendicular to the vertical longitudinal plane of the channel. Zhang et al. [16] investigated the relative permeability of three immiscible fluids flowing in a porous medium. The multi-component multiple-relaxation-time lattice Boltzmann model was used. Akbar et al. [17] numerically analysed the heat and mass transfer of the unsteady MHD flow of a nanofluid through a porous horizontal channel filled with a porous medium. The applied magnetic field was homogeneous and perpendicular to the channel walls. Projahn and Beer [18] investigated the flow and heat transfer of two immiscible fluids in a concentric/eccentric horizontal annular cylinder. For a wide range of Reynolds numbers, velocity and temperature distributions, local and average thermal conductivity equivalents were determined. Sharma and Manjeet [19] examined the MHD nanofluid flow and heat convection in a horizontal channel between two parallel plates through a porous medium. The temperature of the bottom plate was constant, while that of the top plate was variable. The applied magnetic field was homogeneous and perpendicular to the plates. Khaled and Vafai [20] investigated the improvement of heat transfer during the flow of two immiscible fluids in a horizontal channel. Analytical and numerical combinations of water/oil, mercury/water and water/air were analysed. Kasaeian et al. [21] reviewed the cases of using nanofluids and porous media to improve heat transfer in thermal systems with different structures, flow regimes, and boundary conditions. Umavathi and Anwar Beg [22] investigated the flow and heat transfer under the influence of buoyancy in a vertical rectangular channel. In the channel there were clear and viscous fluids saturated with a porous medium. Umavathi and Chamkha [23] investigated the double-diffusive free and forced convective flow of nanofluids in a vertical channel. They also developed a new mathematical model. Umavathi [24] investigated numerically the double diffusive convective flow in a vertical channel. The channel was filled with a nanofluid which was affected by electric and magnetic fields. Abd Elmabound [25] examined the flow of two immiscible fluids through a vertical semi-corrugated channel with natural convection and influenced by a homogeneous transverse magnetic field. One portion of the channel contained an electrically conductive nanofluid and the other contained a clear non-conductive viscous fluid. Umavathi and Beg [26] presented a detailed theoretical and

numerical study on the flow and heat transfer of two immiscible fluids in a vertical channel. Isothermal conditions of the viscous heating were investigated. Umavathi and Sheremet [27] numerically analysed the heat and mass transfer of a coupled stress nanofluid sandwiched between two viscous fluids. Dogonchi et al. [28] numerically analysed the natural convection heat transfer of a copper-water nanofluid in a porous vertical channel between a hot internal rectangular cylinder and an external cold circular cylinder under the influence of an inclined homogeneous magnetic field. Umavathi and Oztop [29] presented a numerical simulation for the analysis of the influence of electric and magnetic fields on the flow and heat transfer of nanofluids in a vertical channel. The temperatures of the left and right walls of the channel were constant and different. Raju and Ojjela [30] conducted a comparative study on the flow and heat transfer of viscous and Jeffrey nanofluids between two parallel plates with periodical injection/suction and with convective boundary conditions, placed inside a porous medium and influenced by an induced magnetic field, Brownian motion, and thermophoresis. Zhao et al. [31] theoretically studied the magnetic field and interfacial electrokinetic effects on the flow and heat transfer of a nanofluid flowing through a horizontal microchannel. Saeed et al. [32] investigated the heat transfer of the Darcy-Forchheimer MHD hybrid nanofluid flow over a porous stretching cylinder influenced by Brownian motion and thermophoresis. Umavathi and Sheremet [33] analysed the mixed convection in a vertical channel whose left and right thirds were filled with a porous medium. The nanofluids flowed through the left and right thirds, while the viscous fluid flowed through the middle third of the channel.

The present paper analytically examines the MHD flow and heat transfer of two immiscible fluids in a horizontal channel between two parallel walls. The medium inside the channel is porous and the top and bottom halves of the channel have a constant but either different or the same permeability. The nanofluid flows through the bottom half, while the pure fluid (viscous fluid without nanoparticles) flows through the top half. The channel walls are at constant and different temperatures. The applied magnetic field is perpendicular to the channel walls and the applied electric field is perpendicular to the vertical plane of the channel. The fluid flow is caused by the constant pressure drop along the channel.

2. Formulation of the problem

This paper examines the flow and heat transfer of two immiscible fluids in a horizontal channel whose walls are made of two infinite impermeable parallel plates at a distance of 2h from one another, whereby the top plate is at constant temperature T_{w1}, and the bottom plate is at constant temperature T_{w2}. The medium in the channel is porous, while the permeability of the top half of the channel is K_1, and the permeability of the bottom half is K_2. The top half, marked Region-I, is filled with a pure fluid with density ρ_1, viscosity μ_1, specific electrical conductivity σ_1, and thermal conductivity k_1.

The bottom half of the channel, marked Region-II, is filled with a nanofluid with density ρ_{nf}, viscosity μ_{nf}, specific electrical conductivity σ_{nf}, and thermal conductivity of nanofluid k_{nf}. The applied external magnetic field is homogeneous and perpendicular to the channel walls, with intensity B, and the applied external electric field is homogeneous and perpendicular to the vertical plane of the channel, with intensity E.

The Cartesian coordinate system was chosen to analyse the problem so that the *x*-axis is in the dividing plane, the *y*-axis is perpendicular to the channel walls, and the *z*-axis is perpendicular to the longitudinal vertical plane of the channel (Figure 1).

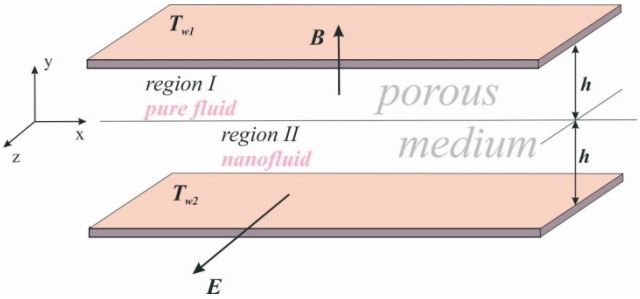

Fig. 1 Physical model

It is assumed that the MHD flow is steady and fully developed and that the fluid properties are constant. It is also assumed that the flow occurs by means of a constant pressure gradient $P = -\partial p / \partial x$ and a constant difference in channel wall temperatures $T_{w1} - T_{w2}$. These assumptions lead to the following equations of motion and energy (Umavathi et al. [6], Petrović et al. [15]):

Region-I

$$P + \mu_1 \frac{\mathrm{d}^2 u_1}{\mathrm{d}y^2} - \frac{\mu_1}{K_1} u_1 - B\sigma_1 \left(E + Bu_1\right) = 0, \tag{1}$$

$$k_1 \frac{\mathrm{d}^2 T_1}{\mathrm{d}y^2} + \mu_1 \left(\frac{\mathrm{d}u_1}{\mathrm{d}y}\right)^2 + \frac{\mu_1}{K_1} u_1^2 + \sigma_1 \left(E + Bu_1\right)^2 = 0 \tag{2}$$

Region-II

$$P + \mu_{nf} \frac{\mathrm{d}^2 u_2}{\mathrm{d}y^2} - \frac{\mu_{nf}}{K_2} u_2 - B\sigma_{nf} \left(E + Bu_2\right) = 0, \tag{3}$$

$$k_{nf} \frac{\mathrm{d}^2 T_2}{\mathrm{d}y^2} + \mu_{nf} \left(\frac{\mathrm{d}u_2}{\mathrm{d}y}\right)^2 + \frac{\mu_{nf}}{K_2} u_2^2 + \sigma_{nf} \left(E + Bu_2\right)^2 = 0 \tag{4}$$

The physical properties of the nanofluid are expressed as follows (Akbar et al. [17]):

$$\begin{gathered} \rho_{nf} = \rho_f \left(1-\phi\right) + \phi\rho_s, \quad \mu_{nf} = \frac{\mu_f}{\left(1-\phi\right)^{2.5}}, \quad \frac{k_{nf}}{k_f} = \frac{k_s + 2k_f - 2\phi\left(k_f - k_s\right)}{k_s + 2k_f + \phi\left(k_f - k_s\right)}, \\ \frac{\sigma_{nf}}{\sigma_f} = 1 + 3\phi\left(\frac{\sigma_s}{\sigma_f} - 1\right)\left(\frac{\sigma_s}{\sigma_f} + 2 - \phi\left(\frac{\sigma_s}{\sigma_f} - 1\right)\right)^{-1} \end{gathered} \tag{5}$$

The boundary conditions and conditions for the dividing plane for velocity and temperature are expressed as follows:

$$\begin{gathered} u_1(h) = 0, \; u_2(-h) = 0, \; u_1(0) = u_2(0), \qquad T_1(h) = T_{w1}, \; T_2(-h) = T_{w2}, \; T_1(0) = T_2(0), \\ \mu_1 \frac{du_1}{dy}(0) = \mu_{nf} \frac{\mathrm{d}u_2}{\mathrm{d}y}(0), \qquad\qquad k_1 \frac{\mathrm{d}T_1}{\mathrm{d}y}(0) = k_{nf} \frac{\mathrm{d}T_2}{\mathrm{d}y}(0). \end{gathered} \tag{6}$$

Equations (1), (2), (3), and (4) and conditions (6) constitute the mathematical model of the presented problem.

The following dimensionless quantities are introduced:

$$y^* = \frac{y}{h},\ u_i^* = \frac{u_i}{U_0},\ \theta_i = \frac{T_i - T_{w2}}{T_{w1} - T_{w2}};\ i = 1,2 \quad , \tag{7}$$

reference velocity U_0 is, for now, arbitrary, and can be mean velocity, maximum velocity or some other, which will be further defined in the paper.

The previous equations are now transformed into the following dimensionless equations:

Region-I

$$\frac{\mathrm{d}^2 u_1}{\mathrm{d}y^2} - R_1^2 u_1 = KHa^2 - P_1, \tag{8}$$

$$\frac{\mathrm{d}^2 \theta_1}{\mathrm{d}y^2} + Br\left[\left(\frac{\mathrm{d}u_1}{\mathrm{d}y}\right)^2 + \Lambda_1 u_1^2 + Ha^2\left(K + u_1\right)^2\right] = 0 \tag{9}$$

where:

$R_1 = \sqrt{\Lambda_1 + Ha^2}$, $\mathrm{P}_1 = \dfrac{Ph^2}{\mu_1 U_0}$, while the 'star' symbol for the dimensionless quantity is omitted for simplicity of notation.

Region-II

$$\frac{\mathrm{d}^2 u_2}{\mathrm{d}y^2} - R_2^2 u_2 = m\left(\frac{K}{n} Ha^2 - P_1\right), \tag{10}$$

$$\frac{\mathrm{d}^2 \theta_2}{\mathrm{d}y^2} + Br\left[\frac{k}{m}\left(\frac{\mathrm{d}u_2}{\mathrm{d}y}\right)^2 + R_3 u_2^2 + R_4 u_2 + R_5\right] = 0 \tag{11}$$

where:

$$\begin{gathered} m = \frac{\mu_1}{\mu_{nf}},\ n = \frac{\sigma_1}{\sigma_{nf}},\ k = \frac{k_1}{k_{nf}},\ R_2 = \sqrt{\Lambda_2 + \frac{m}{n} Ha^2}, \\ R_3 = k\left(\frac{\Lambda_2}{m} + \frac{Ha^2}{n}\right),\ R_4 = 2\frac{k}{n} KHa^2,\ R_5 = \frac{k}{n} K^2 Ha^2 = 2KR_4 \end{gathered} \tag{12}$$

and the 'star' symbol is omitted for the same reason as with Region-I.

In their dimensionless form, conditions (6) are written as

$$\begin{gathered} u_1(1) = 0,\ u_2(-1) = 0,\ u_1(0) = u_2(0), \quad \theta_1(1) = 1,\ \theta_2(-1) = 0,\ \theta_1(0) = \theta_2(0), \\ m\frac{\mathrm{d}u_1}{\mathrm{d}y}(0) = \frac{\mathrm{d}u_2}{\mathrm{d}y}(0), \qquad\qquad k_1\frac{\mathrm{d}\theta_1}{\mathrm{d}y}(0) = \frac{\mathrm{d}\theta_2}{\mathrm{d}y}(0). \end{gathered} \tag{13}$$

Equations (8), (9), (10), and (11) and conditions (13) constitute the mathematical model of the presented problem in its dimensionless form.

3. Solution

Further analysis of the problem requires equations (8), (9), (10), and (11) to be solved with boundary conditions (13). The solution of equations (8) and (9) yields distributions of the dimensionless velocity and the dimensionless temperature in Region-I:

$$u_1(y) = C_1 \exp(R_1 y) + C_2 \exp(-R_1 y) + A, \tag{14}$$

$$\Theta_1(y) = -Br[\frac{C_1^2}{2}\exp(2R_1 y) + \frac{C_2^2}{2}\exp(-2R_1 y) + R_6 \exp(R_1 y) + R_7 \exp(-R_1 y) + R_8 y^2 + C_3 y + C_4] \tag{15}$$

where:

$$A = \frac{P_1 - KHa^2}{R_1^2},\ R_6 = 2C_1\left(A + K\frac{Ha^2}{R_1^2}\right),\ R_7 = 2C_2\left(A + K\frac{Ha^2}{R_1^2}\right),\ R_8 = \frac{1}{2}\left[A^2 R_1^2 + KHa^2(2A + K)\right], \tag{16}$$

while C_1, C_2, C_3 and C_4 are constants of integration to be determined.

The solution of equations (11) and (12) yields distributions of the dimensionless velocity and the dimensionless temperature in Region-II, which are expressed as follows:

$$u_2(y) = C_5 \exp(R_2 y) + C_6 \exp(-R_2 y) + A_1 \tag{17}$$

$$\Theta_2(y) = -Br[R_9 C_5^2 \exp(2R_2 y) + R_9 C_6^2 \exp(-2R_2 y) + R_{10} C_5 \exp(R_2 y) + R_{10} C_6 \exp(-R_2 y) + R_{11} y^2 + C_7 y + C_8] \tag{18}$$

where:

$$A_1 = \frac{m}{R_2^2}\left(P_1 - \frac{K}{n}Ha^2\right),\ R_9 = \frac{1}{4R_2^2}\left(\frac{k}{m}R_2^2 + R_3\right),\ R_{10} = \frac{1}{R_2^2}(2A_1 R_3 + R_4),\ R_{11} = \frac{1}{2}(A_1(R_4 + A_1 R_3) + R_5), \tag{19}$$

and C_5, C_6, C_7 and C_8 are constants of integration.

The Nusselt numbers are given by the following expressions for the top and bottom plates, respectively:

$$Nu_1 = -\left(\frac{\mathrm{d}\theta_1}{\mathrm{d}y}\right)_{y=1} = Br[R_1 C_1^2 \exp(2R_1) - R_1 C_2^2 \exp(-2R_1) + R_1 R_6 \exp(R_1) - R_1 R_7 \exp(-R_1) + 2R_8 + C_3] \tag{20}$$

and

$$Nu_2 = -\frac{k_{nf}}{k_f}\left(\frac{\mathrm{d}\theta_2}{\mathrm{d}y}\right)_{y=-1} = Br\frac{k_{nf}}{k_f}[2R_2 R_9 C_5^2 \exp(-2R_2) - 2R_2 R_9 C_6^2 \exp(2R_2) + R_2 R_{10} C_5 \exp(-R_2) - R_2 R_{10} C_6 \exp(R_2) - 2R_{11} + C_7]. \tag{21}$$

These operations determine distributions of the dimensionless velocity and the dimensionless temperature of the fluids in the channel, with a note that $u_1(y)$ and $\theta_1(y)$ have the dimensionless variable $y \in [0,1]$, whereas $u_2(y)$ i $\theta_2(y)$ have the dimensionless variable $y \in [-1,0]$.

4. Analysis of the results

This section presents a portion of the obtained results for the case when the top half of the channel contains oil, and the bottom half contains a water-based nanofluid. The results are given for the value of P_1=1, the same as in the study by Lohrasbi and Sahai [34]. By choosing P_1=1, the reference velocity in the form of

$$U_0 = \frac{h^2}{\mu_1} P \tag{22}$$

was also chosen, which means that it is directly related to the pressure gradient in this fluid flow.

Cases of copper-water and aluminium oxide (alumina)-water nanofluids were considered. The physical properties of water, oil, and nanoparticles (Das et al. [11]) shown in Table 1 were used.

Table 1 Physical properties of water and nanoparticles

Physical properties	Water (H_2O)	Oil	Copper (C_u)	Aluminium oxide (Al_2O_3)
ρ (kg/m^3)	997.1	900	8933	3970
c_p (J/(kgK))	4179	1800	385	765
K (W/(Km))	0.613	0.15	401	40
σ (S/m)	$5.5 \cdot 10^{-6}$	$3 \cdot 10^{-7}$	$59.6 \cdot 10^{6}$	$35 \cdot 10^{6}$
μ (Pas)	0.001	0.5	-	-

Figures 2 and 3 show the velocity and temperature distributions for different Hartmann number (Ha) values. It should be noted that a change in Ha of the fluid in the upper region of the channel causes a change in Ha of the fluid in the lower region. In the considered case, the bottom half of the channel has lower permeability than the top half.

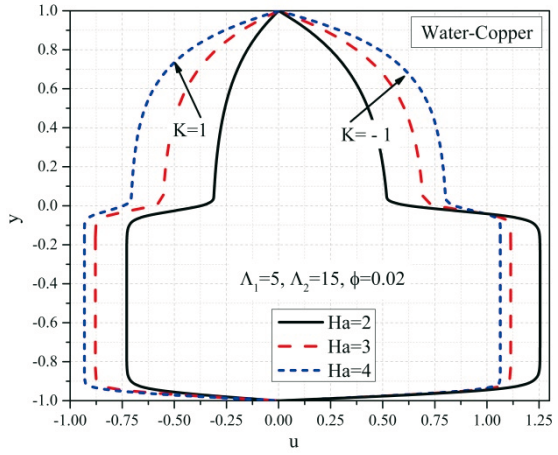

Fig. 2 Velocity distribution for different values of Ha and K

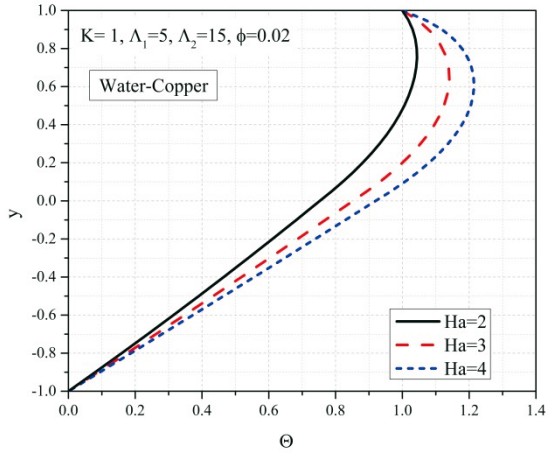

Fig. 3 Temperature distribution for different values of Ha

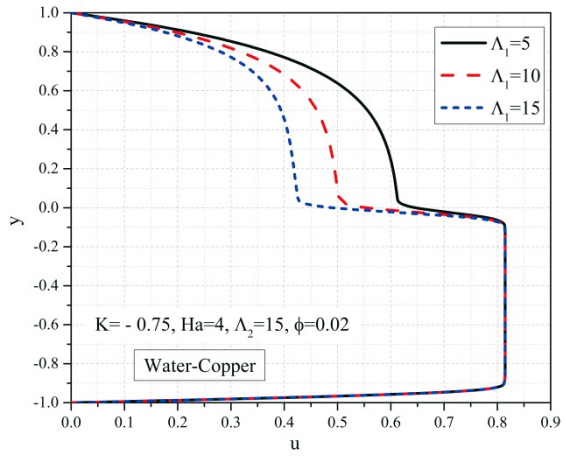

Fig. 4 Velocity distribution for different values of Λ_1

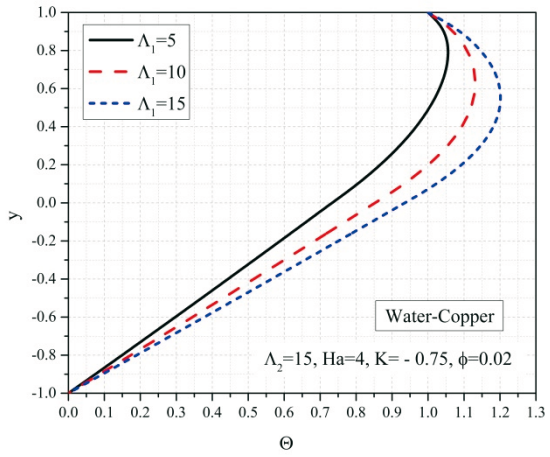

Fig. 5 Temperature distribution for different values of Λ_1

The top half of the channel contains oil, and the bottom half contains a copper-water nanofluid. The value K>0 corresponds to channel operation in the generator mode, while the value K<0 corresponds to channel operation in the magnetic drive pump mode. Figure 2 indicates that higher H*a* values correspond to higher velocity intensities in the upper region for both operating modes of the channel. The lower region exhibits a pronounced flattening of the velocity profile because, owing to the presence of a nanofluid, its H*a* value is significantly higher, and its medium is three times less permeable. As the H*a* value in the lower region increases, the velocity either decreases or increases depending on the channel's operating mode. The interface demonstrates a significant influence of H*a* on the velocity gradient. An increased H*a* value leads to the increase in the tangential stress on the top wall in both operating modes of the channel, whereas the tangential stress on the bottom wall depends on the channel's operating mode.

Figure 3, which shows the results for the channel's generator mode, indicates that an increase in H*a* raises the fluid temperature in the channel. The reason for this is the increase in Joule heating with the increase in H*a*, caused by the Lorentz force. As the H*a* value increases, so does the convective transport of the fluid on the channel walls, which is confirmed by the Nusselt number values shown in Table 2. These conclusions also apply when the channel operates in the pump mode.

Figures 4 and 5 show the velocity and temperature distributions for different values of porosity factor Λ_1, i.e., for different permeabilities of the upper region of the channel. Permeability of the lower region was maintained constant. Figure 4 indicates that an increase in the upper region's porosity factor, i.e., a decrease in its permeability, leads to the flattening of the velocity profile in that part of the channel as well, while the influence on the fluid velocity distribution in the lower region is negligible. The increase in Λ_1 causes a reduction in the tangential stress on the top wall.

Figure 5 indicates that an increase in Λ_1 causes an increase in temperature in the channel because of the increase in the generated heat due to additional energy expended to overcome the resistance of the porous matrix, which is then transformed into heat. The convective heat transfer between the fluid and the channel walls also increases, as indicated by the values of the Nusselt numbers shown in Table 2.

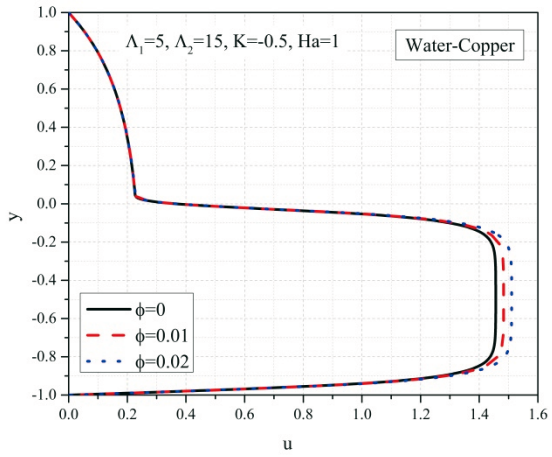

Fig. 6 Velocity distribution for different values of ϕ

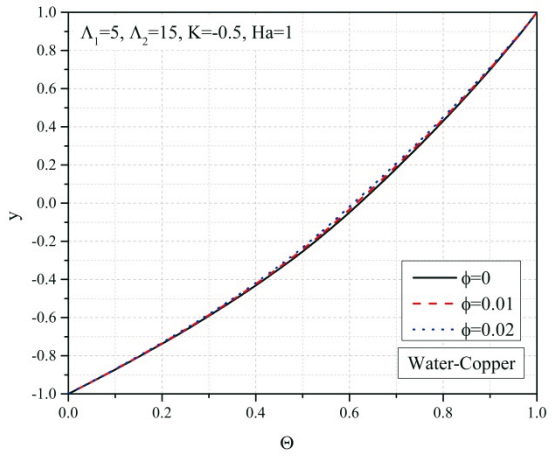

Fig. 7 Temperature distribution for different values of ϕ

Figures 6 and 7 show the velocity and temperature distributions for different values of copper nanoparticle volume concentrations for the case when the channel operates in the pump mode. Figure 6 indicates that an increase in ϕ increases the velocity in the lower region and slightly increases the tangential stress on the bottom wall and the velocity gradient at the interface. This occurs because the increase in the copper nanoparticle concentration leads to an increase in the nanofluid's electrical conductivity and subsequently in the increase in the Lorentz force acting upon it. Changes in the velocity distribution in the upper region of the channel are negligible.

Figure 7 indicates that the temperature in the channel drops, which is caused by an increase in the nanofluid's thermal conductivity following an increase in the copper nanoparticle concentration. The convective heat transfer between the fluid and the channel walls increases with an increase in the copper nanoparticle concentration, as indicated by the values of the Nusselt numbers shown in Table 2.

Figures 8 and 9 show the velocity and temperature distributions for different values of ϕ when the upper region of the channel contains oil and the lower region contains an aluminium oxide-water nanofluid, while the channel operates in the pump mode. The conclusions made for the case of the copper-water nanofluid in the lower region also apply here.

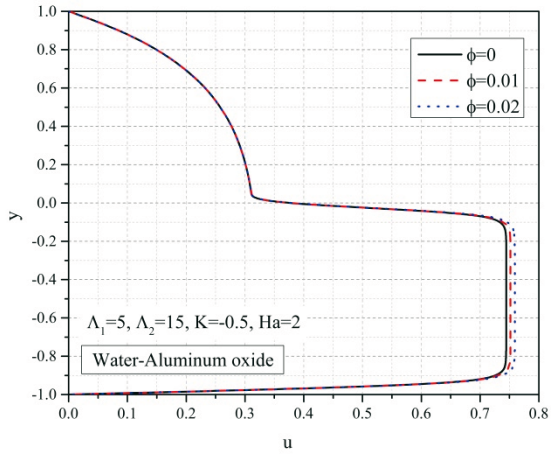

Fig. 8 Velocity distribution for different values of ϕ

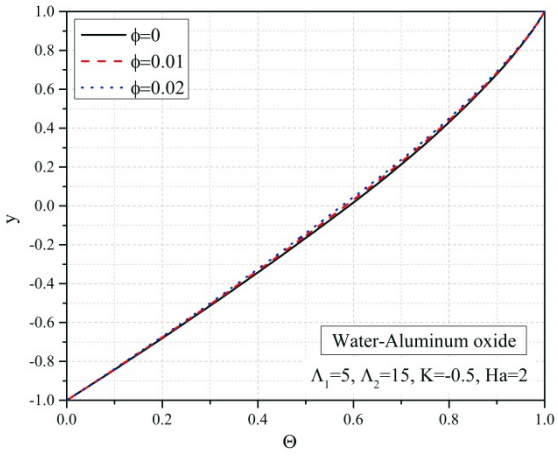

Fig 9 Temperature distribution for different values of ϕ

Figures 10 and 11 show the velocity and temperature distributions for different values of porosity factor Λ_2, when the channel operates in the magnetic drive pump mode. Figure 10 indicates that an increase in the porosity factor reduces the fluid velocity in the lower region of the channel and slightly reduces tangential stresses on the channel walls. Velocity is reduced because a portion of the fluid energy is expended on overcoming the resistance of the porous matrix, after which porous matrix becomes denser in the lower region as Λ_2 increases. Changes in the velocity distribution in the upper region are negligible. The conclusions drawn from the analysis of the temperature distribution with the changes in porosity factor Λ_2 are the same as those drawn when porosity factor Λ_1 was analysed.

Figures 12 and 13 show the velocity and temperature distributions for different values of resistance coefficient K, respectively. The analysis of the influence of the resistance factor is particularly significant when it is different from zero (its value defines the system as a generator, a flow meter, or a pump) and H*a* is constant. The introduction of coefficient K, at a constant value of H*a*, changes the relationship between the pressure gradient and the mean velocity flow/mean flow rate. When K=0 (short-circuited channel), the external electric field acts as an additional pressure gradient.

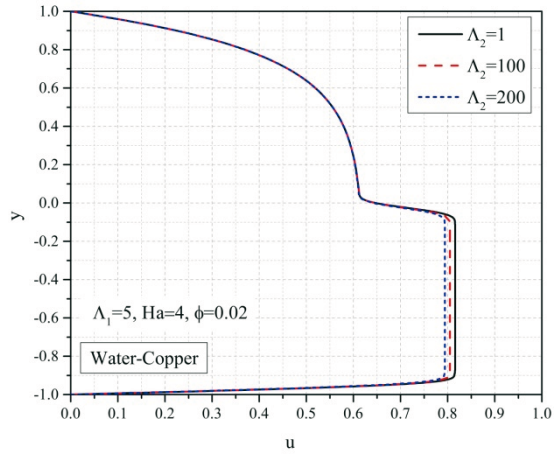

Fig. 10 Velocity distributions for different values of Λ_2

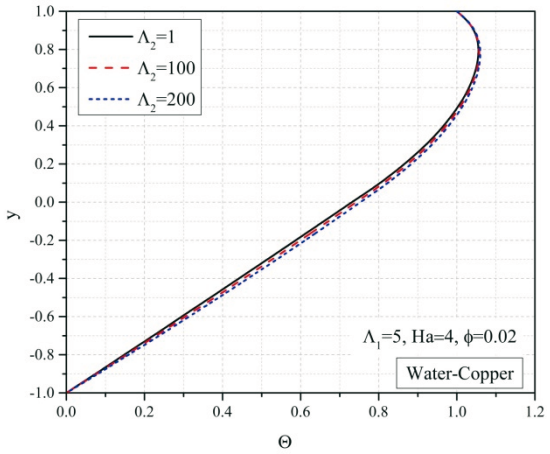

Fig. 11 Temperature distributions for different values of Λ_2

Figure 12 indicates that a change in the value of K can alter the direction of fluid flow in the channel. The influence of fluid interaction at the interface increases with an increase in the absolute value of the loading factor. Higher values of $|K|$ also increase the fluid velocities in the channel and tangential stresses on the channel walls. The velocities in the bottom half of the channel are considerably higher than those in the top half. Owing to higher H*a* values, the velocity profiles in the bottom half of the channel are flattened.

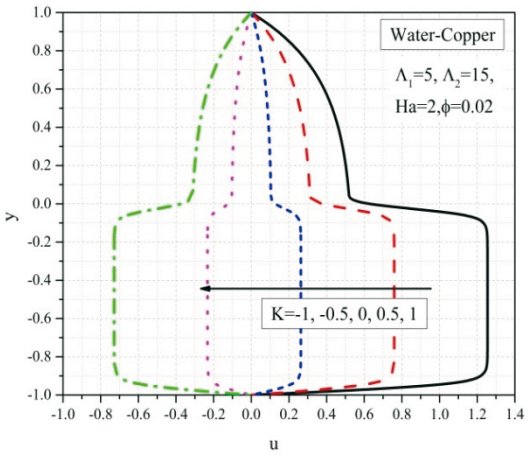

Fig. 12 Velocity distributions for different values of K

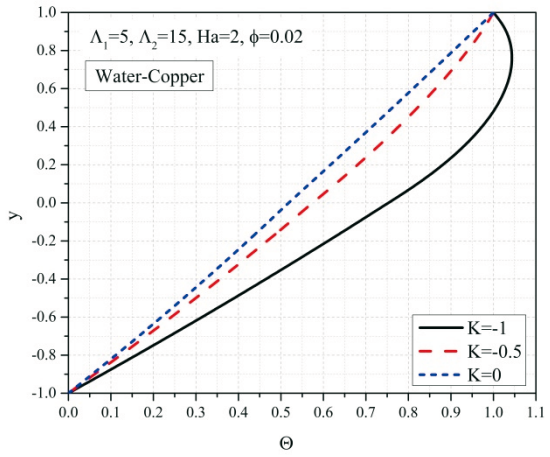

Fig. 13 Temperature distributions for different values of K

Figure 13 indicates that, when the channel is short-circuited, the fluid temperature resembles a straight line in both regions, i.e., the conductive heat transfer prevails. The fluid temperatures in the top half of the channel are higher than those in the bottom half. Higher values of $|K| \neq 0$ also increase the convective heat transfer between the fluid and the channel walls, as indicated by the values of the Nusselt numbers shown in Table 2.

Table 2 Nusselt numbers at the channel walls

Λ_1	Λ_2	Ha	K	ϕ	Nu_1	Nu_2
5	15	2	-1	0.02	0.4262	-0.8899
5	15	3	-1	0.02	1.0579	-0.9860
5	15	4	-1	0.02	1.6508	-1.0658
5	15	4	-0.75	0.02	0.7122	-0.8338
10	15	4	-0.75	0.02	0.9496	-0.9607
15	15	4	-0.75	0.02	1.1200	-1.0484
5	15	1	-0.5	0	-0.3055	-0.8045
5	15	1	-0.5	0.01	-0.3124	-0.8208
5	15	1	-0.5	0.02	-0.3192	-0.8370
5	15	2	-1	0.02	0.4262	-0.8899
5	15	2	-0.5	0.02	-0.2421	-0.6698
5	15	2	0	0.02	-0.4679	-0.5995
5	15	2	0.5	0.02	-0.2511	-0.6788
5	15	2	1	0.02	0.4083	-0.9078
5	1	4	-0.75	0.02	0.7106	-0.8290
5	100	4	-0.75	0.02	0.7216	-0.8628
5	200	4	-0.75	0.02	0.7324	-0.8960

Table 2 shows the local Nusselt numbers Nu_1 and Nu_2 along the upper wall and along the lower wall, respectively. They represent the relations between convective and conductive heat transfer through these walls. The magnification of any of the introduced factors Λ_1, Λ_2, ϕ, or Ha increases the convective heat transfer to the walls of the channel. Magnification $|K| \neq 0$ also increases the convective heat transfer to the walls. Note that $Nu_2<0$, which means that the nanofluid works as a refrigerant.

5. Verification of the results

To compare the results obtained here, we used the problem of the flow and heat transfer of two immiscible Newtonian fluids in an inclined channel influenced by an electric and a magnetic field as investigated by Malashetty et al. [35]. Their results for graphically represented dimensionless velocity were used for the case when the channel inclination angle equalled zero, i.e., when the channel was horizontal, and the thicknesses of fluid layers were equal. To verify the results, the problem considered in the present study was reduced so that the following values were used for the introduced parameters: $\Lambda_1=0$, $\Lambda_2=0$, $\phi=0$, k=0, n=0.5, m=0.5, K= – 1, Ha=2, and $P_1=5$. In this way, the analysed problem was reduced to the problem examined in Malashetty et al. [35].

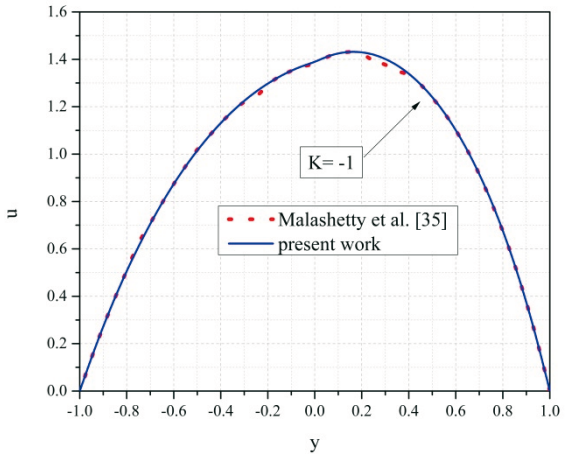

Fig. 14 Velocity comparison

Figure 14 shows the graphic distributions of dimensionless velocity obtained in the present study and in Malashetty et al. [35]. The two distributions almost completely overlap, with a small difference not exceeding 2%. The slight overlap difference is due to the fact that the present study relies on exact methods to solve differential equations, whereas Malashetty et al. [35] used the approximate perturbation technique. Additionally, the diagram values were used for the distribution from [35] when drawing the graph. The slight difference in distributions is fully acceptable.

6. Conclusion

This paper analysed the EMHD flow of two immiscible fluids – a Newtonian fluid and a nanofluid – through a horizontal channel. The permeabilities of the upper and lower channel regions were different. The upper region was saturated with the Newtonian fluid, whereas the lower region was saturated with the nanofluid. The study determined velocity and temperature distributions as well as the Nusselt numbers. The velocity and temperature distributions are graphically represented, while the Nusselt numbers are given in a table as functions of different physical parameters and analysed. The analysis yielded the following conclusions.

As the Hartmann number increases, the velocity in the upper region increases for both channel modes, while in the lower region it increases when the channel operates in the generator mode and decreases when the channel operates in the pump mode. In both cases there is a significant alignment of the velocity profile in the lower part. The temperature in the channel rises.

Increasing the porosity factor in the upper region of the channel aligns the velocity profile in that part, reduces the tangential stress on the upper wall and increases the temperature in the channel.

Increasing the volume fraction of nanoparticles increases the velocity in the lower region and reduces the temperature in the channel.

Increasing the porosity factor in the lower region of the channel reduces the velocity in it and increases the temperature in the channel.

Changing the value of the external electric load factor changes the intensity of the velocity in the channel and can also change the direction of flow. Increasing the absolute value of this factor increases the velocity in the channel and decreases the temperature.

Changes in the value of any of the introduced factors lead to a change in the Nusselt numbers.

REFERENCES

[1] H. Darcy (1856), Les fontaines publiques de la ville de Dijon, Victor Dalmont, Paris

[2] S. U. S. Choi (1995), Enhancing thermal conductivity of fluids with nanoparticles, Developments and Applications of Non-Newtonian Flows, MD vol. 231 and FED vol. 66. ASME, pp. 95-105

[3] Scercliff J. A. (1965), A text Book of Magnetohydrodynamics, London, Pergamon Press

[4] S. K. Das, S. U. S. Choi, W. Yu, T. Pradeep (2007), Nanofluids: Science and Technology, Wiley-interscience, A John Wiley and Sons, INC Publication

[5] Xiang-Qi Wang, Arun S. Mujumdar (2007), Heat transfer characteristics of nanofluids: a review, International Journal of Thermal Sciences 46, pp. 1-19, https://doi.org/10.1016/j.ijthermalsci.2006.06.010

[6] J. C. Umavathi, Ali J. Chamkha, Abdul Mateen and J. Prathap Kumar (2008), Unsteady magnetohydrodynamic two fluid flow and heat transfer in a horizontal channel, Heat and Technology, Vol. 26, No.2, pp. 121-133

[7] Milica Nikodijević, Živojin Stamenković, Jelena Petrović and Miloš Kocić (2020), Unsteady fluid flow and heat transfer trough a porous medium in a horizontal channel with an inclined magnetic field, Transactions of Famena, Vol. 44, No. 4, pp. 31–46, https://doi.org/10.21278/TOF.444014420

[8] Rama Subba Reddy Gorla, Ali Chamka (2011), Natural Convective Boundary Layer Flow over a Horizontal Plate Embedded in a Porous Medium Saturated with a Nanofluid, Journal of Modern Physics, 2, pp. 62-71, https://doi.org/10.4236/jmp.2011.22011

[9] T. Linga Raju and V. Gowrisankara Rao (2021), Effect of Hall currents on unsteady magnetohydrodynamic two – ionized fluid flow and heat transfer in a channel, Int. J. of Applied Mechanics and Engineering, vol.26, No.2, pp. 84 – 106, https://doi.org/10.2478/ijame–2021–0021

[10] Sadegh Khalili, Saeed Dinarvand, Reza Hosseini, Hassein Tamim and Ioan Pop (2014), Unsteady MHD flow and heat transfer near stagnation point over a stretching/shrinking sheet in porous medium filled with a nanofluid, Chin. Phys. B, Vol. 23, No. 4, 048203 https://doi.org/10.1088/1674-1056/23/4/048203

[11] S. Das, A. S. Banu, R. N. Jana, O. D. Makinde (2015), Entropy analysis on MHD pseudo-plastic nanofluid flow through a vertical porous channel with convective heating, Alexandia Engineering Journal https://doi.org/10.1016/j.aej.2015.05.003

[12] S. Das, R. N. Jana, O.D. Makinde (2015), Mixed convective magnetohydrodynamic flow in a vertical channel filled with nanofluids, Engineering Science and Technology, an International Journal https://doi.org/10.1016/j.jestch.2014.12.009

[13] J. A. Lima, G. E. Assad and H. S. Pai (2016), A simple approach to analyze the fully developed two – phase magnetoconvection type flows in inclined parallel – plate channels, Latin American Applied Research, 46:93-98, https://doi.org/10.52292/j.laar.2016.333

[14] Manjeet and Mukesh Kumar Sharma (2020), MHD flow heat convection in a channel filled with two immiscible newtionion and nanofluid fluids, JP Journal of Heat and Mass Transfer, Vol.21, No.1, pp.1-21, https://doi.org/10.17654/HM021010001

[15] J. Petrović, Ž. Stamenković, M. Kocić, M. Nikodijević (2016), Porous medium magnetohydrodynamic flow and heat transfer of two immiscible fluids, Thermal Science, Vol. 20, Suppl. 5, pp. S1405-S1417, https://doi.org/10.2298/ TSCI16S5405P

[16] Da Zhang, Sufen Li, Si Jiao, Yan Shang, Ming Dong (2019), Relative permeability of three immiscible fluids in random porous media determined by the lattice Boltzmann method, International Journal of Heat and Mass Transfer 134, pp.311-320, https://doi.org/10.1016/j.ijheatmasstransfer.2019.01.023

[17] Muhammad Zubair Akbar, Muhammad Ashrof, Muhammad Farooq Iqbal and Kashif Ali (2016), Heat and mass transfer analysis of unsteady MHD nanofluid flow through a channel with moving porous walls and medium, AIP Advances 6, 045222, https://doi.org/10.1063/ 1.4945440

[18] U. Projahn and H. Beer (1987), Thermogravitational and thermocapillary convection heat transfer in concentric and eccentric horizontal, cylindrical annuli filled with two immiscible fluids, Int. J. Heat Mass Transfer, Vol.30, No.1, pp. 93-107, https://doi.org/10.1016/0017-9310(87)90063-9

[19] M. K. Sharma and Manjeet (2017), Nanofluid Flow and Heat Convection in a Channel Filled with Porous Medium, Journal of International Academy of Physical Sciences, Vol. 21, No. 2, pp. 167-188

[20] A. R. A. Khaled and K. Vafai (2014), Heat transfer enhancement by layering of two immiscible co – flows, Internacional Journal of Heat and Mass Transfer 68, pp. 299-309, https://doi.org/10.1016/j.ijheatmasstransfer.2013.09.040

[21] Alibakhsh Kasaeian, Reza Daneshazarian, Omid Mahian, Lioma Kolsi, Ali J. Chamkha, Somchai Wongwises, Ioan Pop (2017), Nanofluid flow and heat transfer in porous media: A review of the latest developments, International Journal of Heat and Mass Transfer 107, pp. 778-791, https://doi.org/101016/j.ijheatmasstransfer.2016.11.074

[22] J. C. Umavathi and O. Anwar Beg (2020), Convective fluid flow and heat transfer in a vertical rectangular duct containing a horizontal porous medium and fluid layer, International Journal of Numerical Methods for Heat and Fluid Flow 0961-5539, https://doi.org/10.1108/HFF-06-2020-0373

[23] J. C. Umavathi and Ali J. Chamkha (2021), Thermo-Solutal Convection of a Nanofluid Utilizing Fourier's-Type Compass Conditions, Journal of Nanofluids 9, No.4, pp. 362-374, https://doi.org/10.1166/jon.2020.1759

[24] J. C. Umavathi (2021), Double diffusive convection in a dissipative electrically conducting nanofluid under ortogonal electrical and magnetic fields: a numerical study, Nanoscience and Technology an International Journal, Vol.12, No.2, pp. 59-90, https://doi.org/10.1615/NanoSciTechnolIntJ.2021036786

[25] Y. Abd Elmaboud (2018), Two layers of immiscible fluids in a vertical semi-corrugated channel with heat transfer: Impact of nanoparticles, Results in Physics, 9, pp. 1643-1655, https://doi.org/10.1016/j.rinp.2018.05.008

[26] J. C. Umavathi and O. Anvar Beg (2020), Effects of thermophysical properties on heat transfer at the interface of two immiscible fluids in vertical duct: Numerical study, International Journal of Heat and Mass Transfer 154(2):119613, https://doi.org/10.1016/j.ijheatmasstransfer.2020.119613

[27] J. C. Umavathi, Mikhail Sheremet (2019), Flow and heat transfer of couple stress nanofluid sandwiched between viscous fluids, International Journal of Numerical Methods for Heat and Fluid Flow, 29(11), pp. 4262-4276, https://doi.org/10.1108/HFF–12–2018–0715

[28] A. S. Dogonchi, M. A. Sheremet, D. D. Ganji, I. Pop (2019), Free convection of copper-water nanofluid in a porous gap between hot rectangular cylinder and cold circular cylinder under the effect of inclined magnetic field, Journal of Thermal Analysis and Calorimetry, 135, pp. 1171-1184, link.springer.com/article/ https://doi.org/10.1007/s10973-018-7396-3

[29] J. C. Umavathi and Hakan F. Oztop (2021), Investigation of MHD and applied electric field effects in a conduit cramed with nanofluids, International Communications in Heat and Mass Transfer, Vol.21:105097, https://doi.org/10.1016/j.icheatmasstransfer.2020.105097

[30] Adigoppula Raju, Odelu Ojjela (2019), Effects of the induced magnetic field, thermophoresis and Brownian motion on mixed convective Jeffrey nanofluid flow through a porous channel, Engineering Reports. WILEY, e212053, https://doi.org/10.1002/eng2.12053

[31] Qingkai Zhao, Hang Xu, Longbin Tao (2020), Flow and heat transfer of nanofluid through a horizontal microchannel with magnetic field and interfacial electrokinetic effects, European Journal of Mechanics/B Fluids 80, pp. 72-79, https://doi.org/10.1016/j.euromechflu.2019.12.003

[32] Anwar Saeed, Asifa Tassaddiq, Arshad Khan, Muhammad Jawad, Wejdan Deebani, Zahir Shah and Saeed Islam (2020), Darcy-Forchheimer MHD Hybrid Nanofluid Flow and Heat Transfer Analysis over a Porous Stretching Cylinder, Coatings 10, 391, https://doi.org/10.3390/coatings10040391

[33] Jawali C. Umavathi, Mikhail A. Sheremet (2020), Heat transfer of viscous fluid in a vertical channel sandwiched between nanofluid porous zones, Journal of Thermal Analysis and Calorimetry https://doi.org/10.1007/s10973-020-09664-1

[34] Lohrasbi J. and Sahai V. (1988), Magnetohydrodynamic heat and transfer in two – phase flow between parallel plates. Applied Scientific Research, 45 (1), 53 – 66, https://doi.org/10.1007/BF00384182

[35] M. S. Malashetty, J. C. Umavathi and J. Prathap Kumar (2021), Two – fluid Magnetoconvection Flow in an Inclined Channel, I. J. Trans. Phenomena, Vol. 3, pp. 73 – 84

Submitted: 14.10.2021

Accepted: 27.6.2022

Jelena Petrović
Faculty of Mechanical Engineering, Niš, Serbia,
jelena.nikodijevic.petrovic@masfak.ni.ac.rs
Živojin Stamenković
Faculty of Mechanical Engineering, Niš, Serbia,
zivojin.stamenkovic@masfak.ni.ac.rs
Jasmina Bogdanović-Jovanović
Faculty of Mechanical Engineering, Niš, Serbia,
jasmina.bogdanovic.jovanovic@masfak.ni.ac.rs
Milica Nikodijević*
Faculty of Occupational Safety, Niš, Serbia
Miloš Kocić
Faculty of Mechanical Engineering, Niš, Serbia,
milos.kocic@masfak.ni.ac.rs
Dragiša Nikodijević
Faculty of Mechanical Engineering, Niš, Serbia,
dragisan@masfak.ni.ac.rs
*Corresponding author:
milica.nikodijevic@znrfak.ni.ac.rs